

# Study on the Tribological Behaviors of Different PEEK Composite Coatings for Use as Artificial Cervical Disk Materials

Jian Song, Zhenhua Liao, Song Wang, Yuhong Liu, Weiqiang Liu, and Rajnesh Tyagi

(Submitted August 26, 2015; in revised form November 14, 2015; published online December 17, 2015)

Poly(ether-ether-ketone) (PEEK) is a type of biomaterial which may be used for modifying the surface of materials used in implants. Hence, in the present investigation, the potentiality of PEEK and its composites coatings has been explored for improving the friction and wear behavior of the Ti6Al4V to be used for cervical disks. The structural characteristics, micro-hardness, friction, and wear characteristics of PEEK/Al<sub>2</sub>O<sub>3</sub> and PEEK/SiO<sub>2</sub> composite coatings have been investigated and compared with pure PEEK coating and bare titanium alloy sample. According to the XRD analysis results, these coated samples were mainly orthorhombic crystalline form. The contact angle values of PEEK and its composite coatings were higher, while micro-hardness values of these samples decreased significantly. The thickness values of the three coated samples were all above 70 μm on average. The average friction coefficients with a counterface of ZrO<sub>2</sub> ball decreased significantly, especially under NCS (newborn calf serum) lubricated condition. After comprehensive evaluation, the PEEK/Al<sub>2</sub>O<sub>3</sub> coating demonstrated optimum tribological properties and could be applied as bearing materials for artificial cervical disk.

**Keywords** artificial cervical disk, PEEK coating, titanium alloy (Ti6Al4V), tribology

## 1. Introduction

Titanium alloys are widely used as bio-implant materials because of their good mechanical properties, prominent biocompatibilities, and corrosion resistance (Ref 1). They are also applied as the preferred endplate materials for artificial cervical disk due to the imaging requirements (e.g., MRI/CT) (Ref 2). However, the poor tribological performances of titanium alloys might cause aseptic loosening and the osteolysis, which could lead to the failure of the replaced cervical disk implants (Ref 3, 4). Thus, it is particularly important to modify the tribological performance of the titanium alloys. Surface modification by coating is an effective means to improve the tribological behavior of titanium alloys without changing the bulk mechanical characteristics (Ref 5).

The tribological properties of titanium alloys modified by coatings have been extensively researched. It has been reported

that many coatings, such as the titanium aluminum nitride (TiAlN) nanocomposite coating (Ref 6), graphite-like carbon coating (Ref 7), and diamond-like carbon coating (Ref 8, 9), could increase the wear resistance of titanium alloys. Furthermore, researchers have shown great interest in surface modifications by polymer coatings. Yang et al. (Ref 10) deposited the Ni-P-PTFE composite coatings on titanium alloy. It was suggested that this coating could obviously promote the tribological properties of titanium alloy. Panjwani et al. (Ref 11) coated the ultra-high molecular weight polyethylene (UHMWPE) thin film onto Ti6Al4V alloy by using dip coating method. The results proved that UHMWPE coating could improve the wear behavior of titanium alloy, which made a low coefficient of friction (0.15) and high wear durability (>96,000 cycles) for the tested conditions. In fact, every coating has its own advantages as well as disadvantages. There are few coatings that combine the toughness of metal, wear resistance of ceramic, and an excellent bonding strength to satisfy the needs, especially in biomedical application (Ref 12).

Poly(ether-ether-ketone) (PEEK) is a special type of semi-crystalline engineering thermoplastic with excellent mechanical, chemical, and physical characteristics (Ref 13) and possesses remarkable biocompatibility, radiation permeability, and other advantages. Thus, its superior comprehensive properties show great potential in the study of the new generation long-life artificial cervical disk. It has been successfully used in the field of interbody fusion cage (Ref 14). However, the disadvantage of PEEK is its poor osseointegration, which can lead to implant stability problems (Ref 15). While titanium and its alloys have shown excellent osseointegration (Ref 16). Hence, the combination of PEEK coating and titanium alloys might be a good idea to make use of their beneficial properties to complement each other. However, in order to make the characteristics of PEEK better, to satisfy the requirements of artificial cervical disk in high precision manufacture, corrosion resistance, wear resistance, and anti-fatigue, PEEK properties

**Jian Song** and **Yuhong Liu**, State Key Laboratory of Tribology, Tsinghua University, Beijing 100084, People's Republic of China; State Key Laboratory of Tribology, Tsinghua University, Beijing 100084, People's Republic of China; **Zhenhua Liao** and **Song Wang**, Department of Mechanical Engineering, Tsinghua University, Beijing 100084, People's Republic of China; Department of Mechanical Engineering, Tsinghua University, Beijing 100084, People's Republic of China; **Weiqiang Liu**, Biomechanics and Biotechnology Lab, Research Institute of Tsinghua University in Shenzhen, Shenzhen 518057, People's Republic of China; and **Rajnesh Tyagi**, Department of Mechanical Engineering, Indian Institute of Technology (BHU) Varanasi, Varanasi 221005, India. Contact e-mails: 575248386@qq.com and weiqliu@hotmail.com.

could be modified through particle filling using materials by adding filler materials which have been clinically proved safe and harmless to human health.

There are very few investigations about PEEK coating being applied as bearing materials for artificial cervical disk. Hence, in this study, the tribological properties of PEEK has been modified by adding alumina ( $\text{Al}_2\text{O}_3$ ) and silicon dioxide ( $\text{SiO}_2$ ) nanoparticles and coated onto the Ti6Al4V alloy plates, aiming to assess the potential of such PEEK composite coatings for being used as artificial cervical disk bearing materials. The wear behavior of these coatings has been explored by using a ball-on-flat apparatus under physiological load in dry friction and 25 wt.% NCS lubricated conditions. The friction and wear characteristics of Ti6Al4V alloy without coating and with pure PEEK coating have been also examined for the purpose of comparison.

## 2. Methods

### 2.1 Sample Preparation

As shown in Table 1, three kinds of coatings were deposited onto Ti6Al4V (TC4, Baoji Titanium Industry Co., Ltd.) plate substrates for surface characterization and tribological testing, respectively. The rectangular shaped Ti6Al4V were 40 mm in length, 20 mm in width and 5 mm in thickness, which were cut from larger panels. The PEEK,  $\text{Al}_2\text{O}_3$  and  $\text{SiO}_2$  particles were supplied by Beijing Sino-Rich Material Technology Co., Ltd. The average size of PEEK particles was below 100  $\mu\text{m}$  and that of  $\text{Al}_2\text{O}_3$  and  $\text{SiO}_2$  particles were about 50 nm. Before coating, 2 wt.%  $\text{Al}_2\text{O}_3$  and 2 wt.%  $\text{SiO}_2$  particles were dispersed into PEEK, respectively. The Ti6Al4V specimens were cleaned in an acetone and deionized water bath for 15 min, respectively. Next, the plates were degreased for 10 min by soaking in a water-based solution of alkaline cleaner and followed by thorough rinsing with deionized water and roughened by sand-blasting to enhance the mechanical bonding of the deposited coatings. Then, the coatings were deposited on the previously treated substrates following the method used by Nunez et al. (Ref 17). Xanthan and morpholine gum were mixed with the pure PEEK particles, PEEK with 2 wt.%  $\text{Al}_2\text{O}_3$  particles and PEEK with 2 wt.%  $\text{SiO}_2$  particles into a liquid dispersion to prohibit rust and inhibit sagging (formation of tears of the deposited coating), respectively. When cured over 350 °C, the gum particles were removed from the coating, leaving only the PEEK composite solid particles in the coating. After being cured, the PEEK composite particles were evenly distributed throughout the thickness of the coating.

**Table 1 The PEEK composite coatings onto Ti6Al4V alloy**

Sample code	Coating	Substrate	Surface roughness, Ra/nm
C0	None	Ti6Al4V alloy	48
C1	PEEK		596
C2	PEEK + 2 wt.% $\text{Al}_2\text{O}_3$		548
C3	PEEK + 2 wt.% $\text{SiO}_2$		831

### 2.2 Surface Layer Characterization

Microstructural examinations of uncoated and coated Ti6Al4V samples were conducted using x-ray diffraction (D8 ADVANCE, BRUKER) analysis. The static-water contact angles were measured under distilled water and 25 wt.% NCS ( $5.0 \pm 0.1$  g/L protein concentration, Zhejiang Tianhang Biotechnology Co., Ltd) lubricant by a contact angle apparatus. Hardness measurements were conducted on the original surfaces of the plates by a micro-hardness tester (Tukon 2500 DM-400) with the indentation load of 0.05 g and loading time of 15 s. In order to measure the thickness of all the coatings, the samples were cut into small pieces and the cross sections were studied by SEM (FEI Quanta 200 FEG) as well as EDX analysis. All experimental results were obtained by averaging the values of at least four repetitions.

### 2.3 Tribological Tests

The tribological properties of all the Ti6Al4V samples were tested against a 6.35 mm diameter zirconia ( $\text{ZrO}_2$ ) ball (having surface roughness  $R_a = 20$  nm and supplied by Haining Kove Bearing Technology Co., Ltd.) using a ball-on-flat apparatus (UMT-3, CETR) under reciprocating motion (Fig. 1). The structure of most artificial cervical disks were designed as the ball-socket joint, and the sliding and rubbing motion of ball-socket articulating surfaces could lead to serious surface wear. So this situation could be simplified as the basic ball-to-flat contact mode (Ref 18).

The tribological tests were conducted under dry friction and 25 wt.% NCS lubricated conditions at the temperature of 37 °C for an hour. According to ISO 18192-1 and ASTM F2423, the motion frequency was chosen as 2 Hz while the reciprocating stroke was 3 mm (nearly the same to the sliding distance of artificial cervical disk) (Ref 3). Hence, the average sliding speed for the test was 12 mm/s. The normal load was chosen as 3.0 N, an equivalent contact stress of  $\sim 472.2$  MPa for bare Ti6Al4V alloy samples, and  $\sim 65.8$  MPa for coated samples based on Hertz contact theory. During the tribological test, the values of load and frictional forces were acquired by a two-dimension sensor simultaneously. Then the friction coefficients were calculated by computer automatically. All experimental results reported here were obtained by averaging the values of at least four repetitions.

The worn surfaces were observed under scanning electron microscopy (FEI Quanta 200 FEG) as well as EDX analysis. Before SEM examination, the samples were cleaned in an acetone and deionized water bath for 15 min and then coated with a thin platinum (Pt) layer to improve image quality. The three-dimensional subsurface damage was observed by a three-dimensional white-light interfering profilometry. Owing to the bumpy surfaces of the samples, it was hard to ensure the accuracy of the wear volume calculation. Thus, only the maximum wear depth and maximum wear width of the wear scars on the plates were measured by the three-dimensional white-light interfering profilometer. All the reported results are obtained by averaging the values of at least four repetitions.

## 3. Results and Discussion

### 3.1 Microstructure and Composition Analysis

Figure 2 displays the XRD analysis on the surface of the bare and coated Ti6Al4V alloys. As reported above, PEEK is a

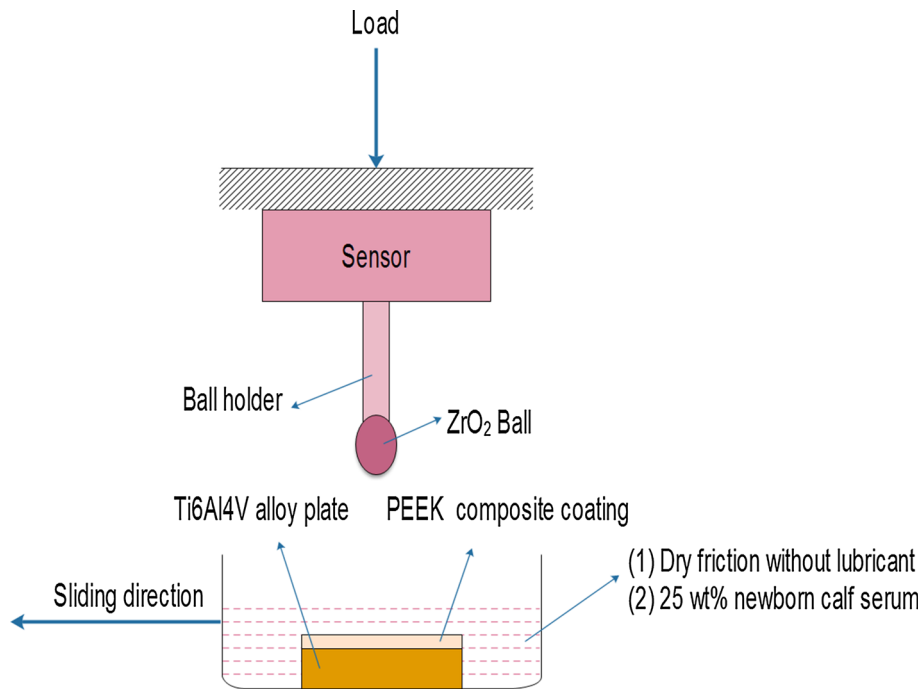


**Fig. 1** Schematic diagram of the loading/motion configuration for a ball-on-flat contact apparatus

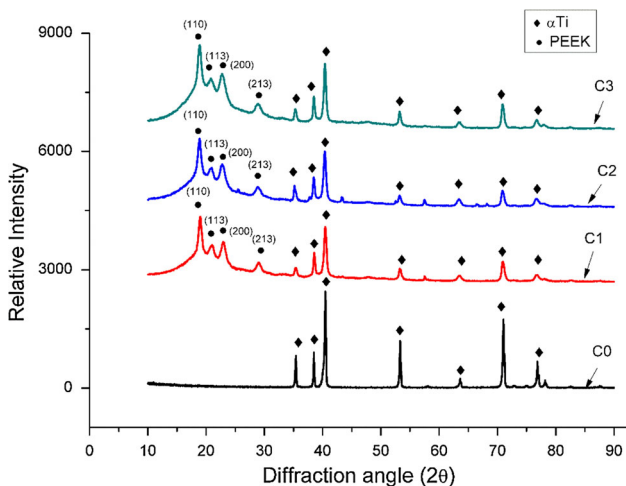


**Fig. 2** XRD patterns of bare and coated Ti6Al4V alloys

semi-crystalline thermoplastic polymer (Ref 13). As shown in Fig. 2, it is suggested that these coated samples are mainly orthorhombic crystalline form (Ref 19). The three peaks around  $2\theta$  of  $20^\circ$  can be assigned to the (110), (113), and (200) planes of crystallized PEEK, respectively. Besides, the peak around  $29^\circ$  is the (213) plane of PEEK. Normally, XRD cannot detect the phases lower than that approximately 5%. Hence, there are no visible peaks corresponding to  $\text{Al}_2\text{O}_3$  and  $\text{SiO}_2$ , which is in agreement with the previous literature (Ref 20).

The static contact angles of bare and coated samples with different liquids are shown in Fig. 3. As shown in Table 1, the bare sample is designated as C0, the one coated with pure PEEK as C1 and those coated with PEEK- $\text{Al}_2\text{O}_3$  and PEEK- $\text{SiO}_2$  are designated as C2 and C3, respectively. It could be seen from Fig. 3 that contact angles of the bare Ti6Al4V alloy

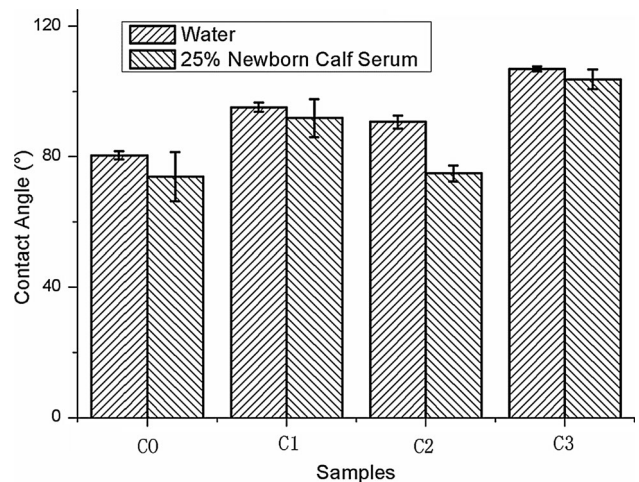


**Fig. 3** The contact angle of bare and coated Ti6Al4V alloys

sample with distilled water and 25 wt.% NCS are approximately  $80.4^\circ$  and  $73.8^\circ$ , respectively. However, compared to C0, the contact angle values of those coated Ti6Al4V alloys with these liquids are all higher which may be attributed to the relatively strong hydrophobicity of PEEK (Ref 21). Besides, compared to the pure PEEK coating, the contact angles of C2 with the two liquids are lower while that of C3 are higher. In essence, C3 sample demonstrates the highest contact angle and the increase reaches to 31.8 and 41.1% for distilled water and 25% NCS lubricant, respectively, in comparison to those observed for bare alloy. Moreover, C3 sample shows a comparable contact angle ( $74.8^\circ$ ) with 25% NCS, compared with the bare one in the same condition. It is defined that water contact angles  $>90^\circ$  are hydrophobic, while water contact angles  $<90^\circ$  are hydrophilic, indicating a good wettability of

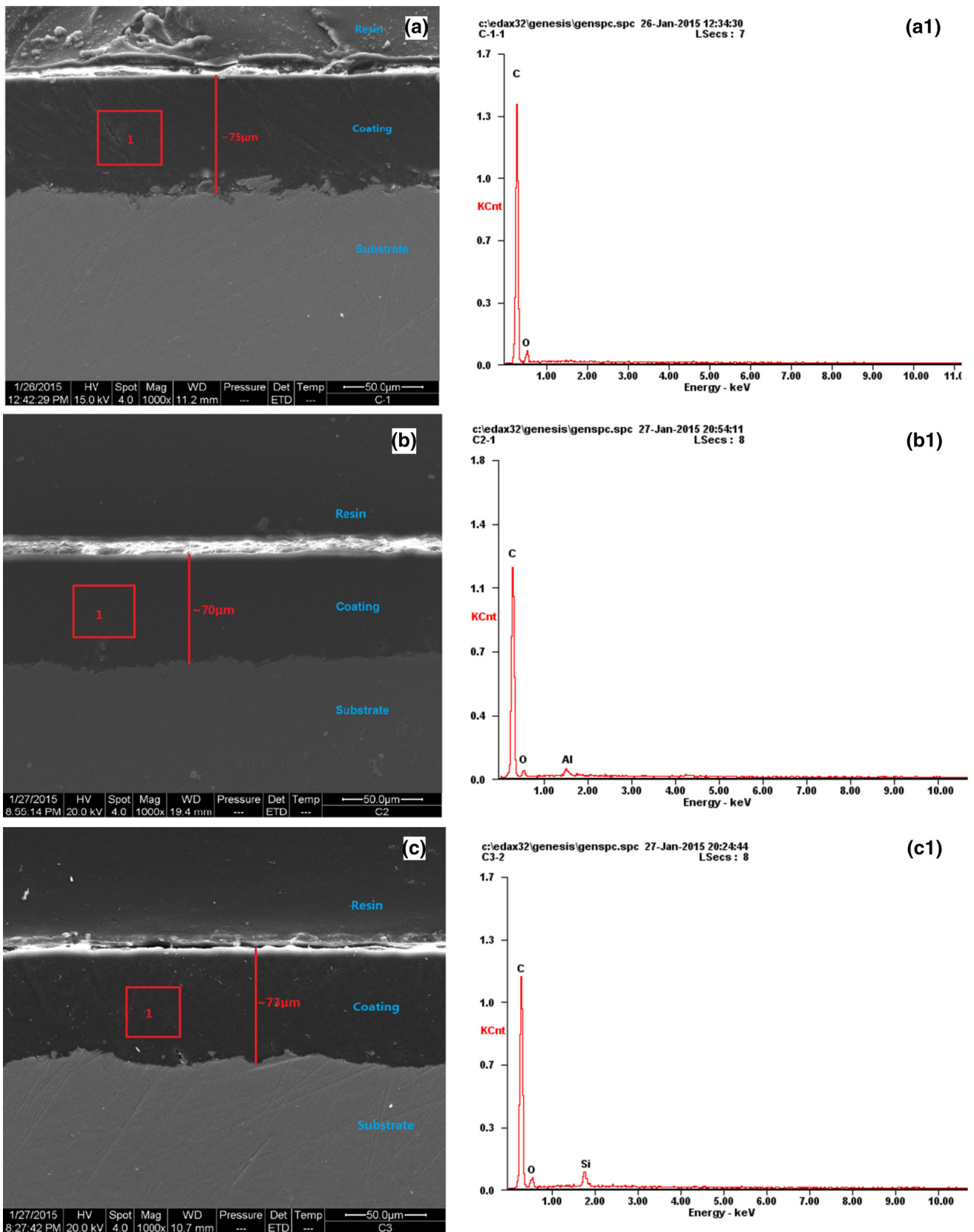


**Fig. 4** The cross section micrograph and EDX analysis for: (a) cross section and thickness micrographs of the PEEK coating, (a1) relative EDX analysis and (b) cross section and thickness micrographs of the PEEK/Al<sub>2</sub>O<sub>3</sub> coating, (b1) relative EDX analysis, and (c) cross section and thickness micrographs of the PEEK/SiO<sub>2</sub> coating, (c1) relative EDX analysis



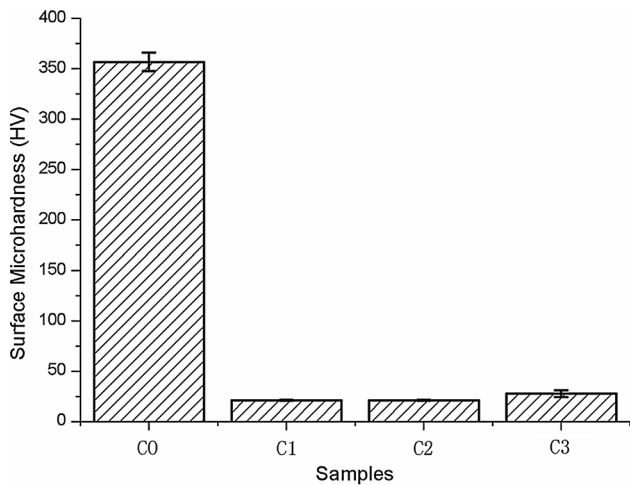


**Fig. 5** The micro-hardness of bare and coated Ti6Al4V alloys

the surface (Ref 22). The obtained results for C2 may be attributed to the hydroxyl groups in  $\text{Al}_2\text{O}_3$  of C2 coating, which are hydrophilic and could improve the wettability of the surface. Though, there are also some hydroxyl groups in  $\text{SiO}_2$  of C3 coating, its surface roughness is higher ( $R_a = 831 \text{ nm}$ ), which might have a strong influence on the wettability of the surface (Ref 23). Hence, the contact angle values of C3 in distilled water and 25% NCS lubricant are the highest among all samples. It is reported that the superior surface wettability could promote the implant surface area for human osteoblast adhesion, which is important to the implant materials (Ref 24). Thus, PEEK/ $\text{Al}_2\text{O}_3$  coating could retain the wettability of original Ti6Al4V alloy preferably. Figure 3 also reveals that the static contact angles with distilled water are relatively larger than those with NCS, especially for C2 sample. The probable reason may be the adsorption of proteins in NCS. Meanwhile, there are some polar groups, such as  $-\text{COO}-$ ,  $-\text{NH}_3$ , and  $-\text{OH}$ , in serum proteins and making the hydrophilic nature of proteins better. This phenomenon indicates that NCS lubricant could cover the sample surface easily and might protect the surface from severe wear and friction.

Figure 4 displays the cross section micrograph and EDX analysis of the PEEK composite coatings. It is observed that the thickness values of coatings in C1, C2, and C3 are about 75, 70, and 73  $\mu\text{m}$ , respectively, which are larger than the similar polymer coatings reported earlier (Ref 11, 25). According to the EDX analysis, the elements in the coatings are in agreement with our sample preparation, which are the component of PEEK, PEEK filled with  $\text{Al}_2\text{O}_3$  and PEEK filled with  $\text{SiO}_2$ , respectively. In addition, no obvious cracks could be found at the interfaces of coatings and substrates as shown in Fig. 4, which ensures a good mechanical bonding and confirms the stability of the PEEK and its composite coatings.

### 3.2 Micro-hardness

The micro-hardness values of the bare and coated Ti6Al4V alloy samples are given in Fig. 5. There is no doubt that the average surface micro-hardness values of all the coated specimens are very less compared to the bare alloy. It is indicated that the micro-hardness value of PEEK coating could be increased about 35% by adding 2 wt.%  $\text{SiO}_2$  nanoparticles. The reason is that when cured, the structure of PEEK/ $\text{SiO}_2$

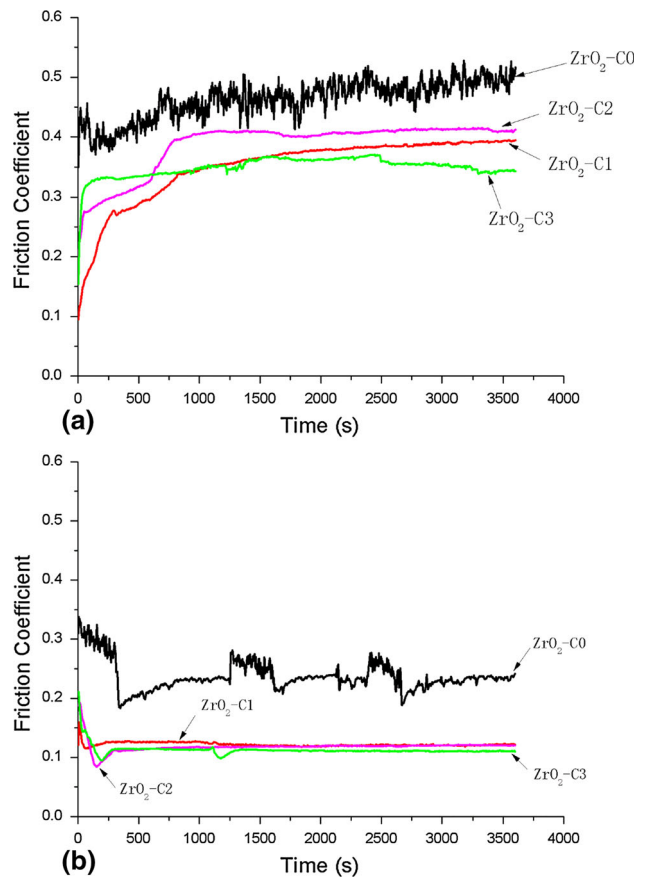


**Fig. 6** Friction coefficient curves for wear test conducted: (a) in dry friction and (b) in 25 wt.% NCS lubricated conditions

coating changes into oversaturated solid solution with respect to  $\text{SiO}_2$  gradually and will make the lattice deformation, making the hardness increase (Ref 26). However, the obtained results reveal that adding 2 wt.%  $\text{Al}_2\text{O}_3$  nanoparticles into PEEK coating could not improve the micro-hardness. There are no obvious differences between the micro-hardness of PEEK ( $20.9 \pm 0.5 \text{ HV}$ ) and PEEK/ $\text{Al}_2\text{O}_3$  ( $21.0 \pm 0.4 \text{ HV}$ ). Hence, in terms of  $\text{Al}_2\text{O}_3$  nanoparticles, the weight percent value of 2% could not make grain refinement and particle strengthening effects notable. Furthermore, the measured results are in agreement with the PEEK coatings on Fe substrate (Ref 27) and higher than that on Al substrate (Ref 28) because of the higher crystallinity level.

### 3.3 Tribological Characteristics

Figure 6 shows the friction curves of four types of samples sliding against  $\text{ZrO}_2$  balls at applied load of 3 N under dry and NCS lubricated conditions. As seen from Fig. 6(a), bare Ti6Al4V alloy displays a considerably high friction coefficient (0.463) in comparison to coated specimens, which sharply increases at the beginning of sliding and fluctuates during the whole test, indicating poor friction resistance. It has been proposed that the high reactivity of titanium makes itself prone to the formation of the surface oxide layer easily. The failure of this surface oxide layer of Ti6Al4V alloy might result in the rise of friction coefficient (Ref 7). The friction coefficient also

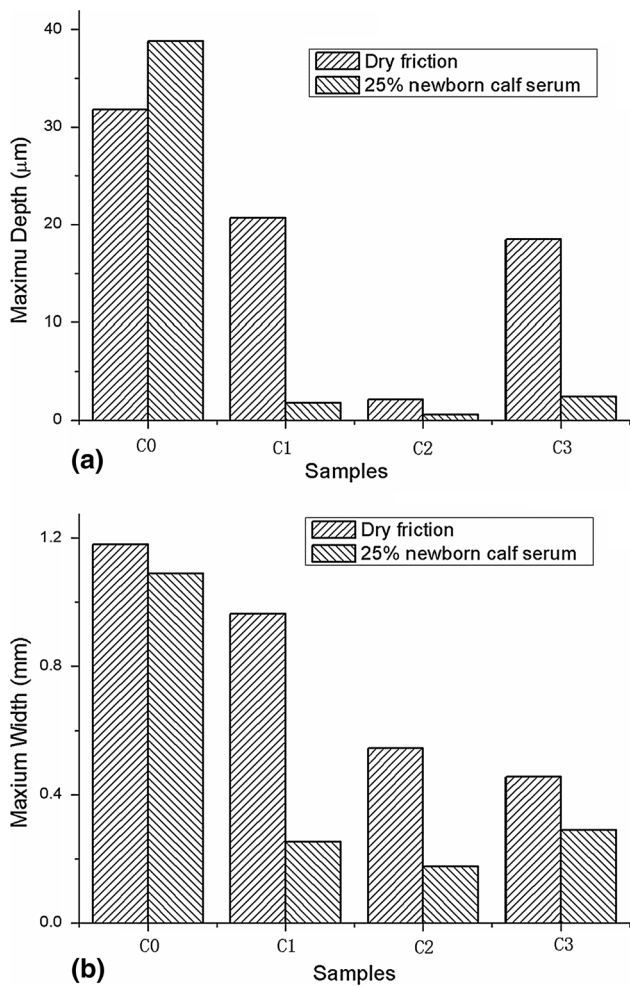


**Fig. 7** The (a) maximum wear depth and (b) maximum wear width for Ti6Al4V plates in dry friction and 25 wt.% NCS lubricated conditions

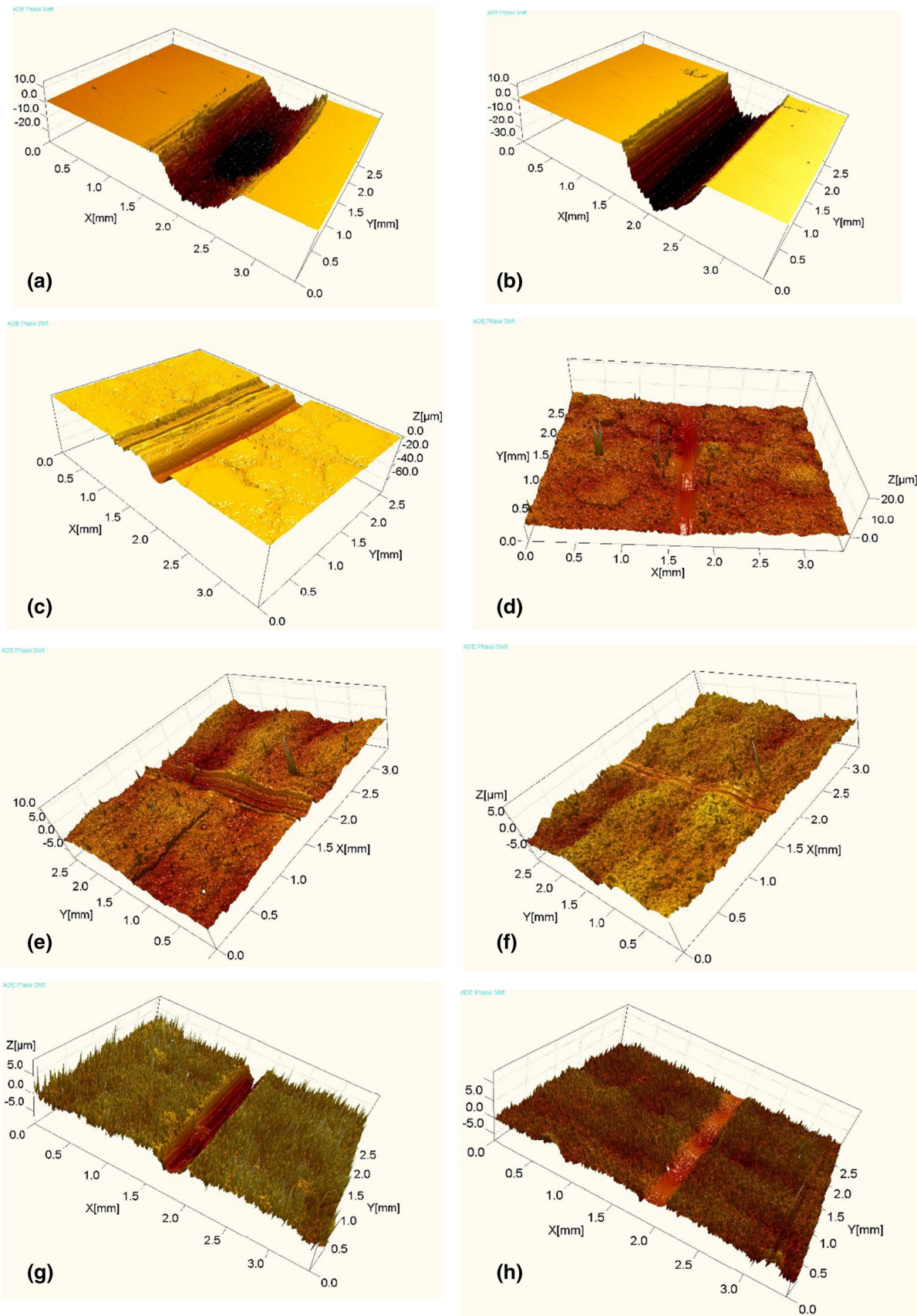
increases sharply in all the coated specimens after certain time but remains stable thereafter. There are no significant differences among the average friction coefficients of C1 (0.351), C2 (0.387), and C3 (0.349) in dry friction condition, while the values are approximately three-fourths of C0. Owing to the NCS lubricant, the average friction coefficients of all samples are about half of those in dry friction condition. As shown in Fig. 6(b), the friction coefficient of C0 still fluctuates but with decreased magnitude in comparison to the dry sliding. It is demonstrated that the friction coefficients of the three coated specimens i.e., C1, C2, C3 are stable and  $< 0.12$  at all the times during the test. There is only a marginal difference among the friction coefficients of the coatings. However, the PEEK/SiO<sub>2</sub> coating has shown the lowest friction coefficient of 0.112. The results suggest that the PEEK and its composite coatings are beneficial in reducing the friction coefficients of Ti6Al4V alloy both in dry friction and NCS lubricated conditions. In addition, the friction coefficients observed in the present study are in the allowable range predicted by the simplified models used for artificial joints (Ref 29-31).

Figure 7 presents the maximum wear depth and the maximum wear width for the four Ti6Al4V alloy plate samples. It is apparent that C0 has the largest maximum wear depth and

maximum wear width both in dry and NCS lubricated conditions, while the C2 has the least. The maximum wear depth of C2 represents a 93.36% decline in dry friction and a 98.53% decline in NCS lubricated condition compared to C0 under the same conditions. Besides, the maximum wear width of C2 also demonstrates an obvious decrease of 53.90% in dry friction and 83.94% in NCS lubricated condition, respectively. Figure 8 illustrates the 3D-profile micrograph of the worn surfaces of different coatings, respectively. It could be seen that the coated surfaces have a higher roughness in comparison to the base alloy. According to the deep and wide grooves seen in Fig. 8(a) and (b), it appears that the surface of uncoated Ti6Al4V alloy substrate has been badly worn. The worn surface of C2 has shown the least wear depth and width both in dry and NCS lubricated conditions which could be observed from Fig. 8(g) and (h) and this is in agreement with the measured results given in Fig. 7.

Micrographs of wear scar examined under SEM for all samples are shown in Fig. 9. It can be seen that there is a significant difference in micrographs among the bare and coated Ti6Al4V alloys. A large amount of wear grooves, cracks, and flake wear debris (white spots in the micrograph) and debris could be seen on the worn surface of base alloy (C0) as evident from Fig. 9(a) and (b), especially in dry friction. Compared with this, wear track of the coated Ti6Al4V alloys are smooth after sliding for an hour as seen in Fig. 9(c)-(h). Specifically, there is no obvious wear scar in Fig. 9(f) corresponding to PEEK-Al<sub>2</sub>O<sub>3</sub> coating under NCS lubricated condition while some adhesive wear scar with a few cracks could be seen on the worn surface of other coatings. In order to further explore the operative wear mechanisms, the compositions of debris particles and wear tracks for the samples both in dry friction and NCS lubricated conditions have also been detected using EDX and the corresponding spectrums are illustrated in Fig. 10 and 11, respectively, for dry and NCS lubricated conditions. EDX analysis of the worn surface of base alloy shows the presence of Zr apart from Ti, Al, and V on the worn surface which reflects the transfer of materials from counterface to the base alloy under dry conditions as seen from Fig. 10(a1). However, while sliding under NCS the EDX spectra of the base alloy does not show any trace of Zr as could be seen from Fig. 11(a1). Surface plowing by the hard mating ZrO<sub>2</sub> ball might be the main reason for the serious damage of bare Ti6Al4V alloy surface both in dry friction and NCS lubricated conditions. Thus, it is noted that the deformation under plowing force as well as abrasive wear and adhesive wear are the main wear mechanisms for bare Ti6Al4V alloy in dry friction condition. While the deformation under plowing force and abrasive wear are the main wear mechanisms for bare Ti6Al4V alloy in NCS lubricated condition.

Because of the protection provided by the coatings, the wear scar observed in Fig. 10(b) is mainly composed of PEEK including C and O elements as shown in Fig. 10(b1). Few debris particles and some fatigue cracks could be seen in the SEM micrograph of C1 in dry friction condition. The compositions of the wear scar observed in Fig. 11(b) are also C and O elements as shown in Fig. 11(b1). However, it is apparent that the worn surface of C1 has been a large amount of adhered particles under NCS lubricated condition. Thus, it is believed that the fatigue wear and mild adhesive wear are the main wear mechanisms for C1 in dry friction condition. While adhesive wear is the main wear mechanism for C1 in NCS lubricated condition. Similar to the C1 sample, the wear scar of



**Fig. 8** The 3D-profile micrographs of the wear scars for: (a) C0 in dry friction condition, (b) C0 in 25 wt.% NCS lubricated condition, (c) C1 in dry friction condition, (d) C0 in 25 wt.% NCS lubricated condition, (e) C2 in dry friction condition, (f) C0 in 25 wt.% NCS lubricated condition, (g) C3 in dry friction condition, and (h) C0 in 25 wt.% NCS lubricated condition



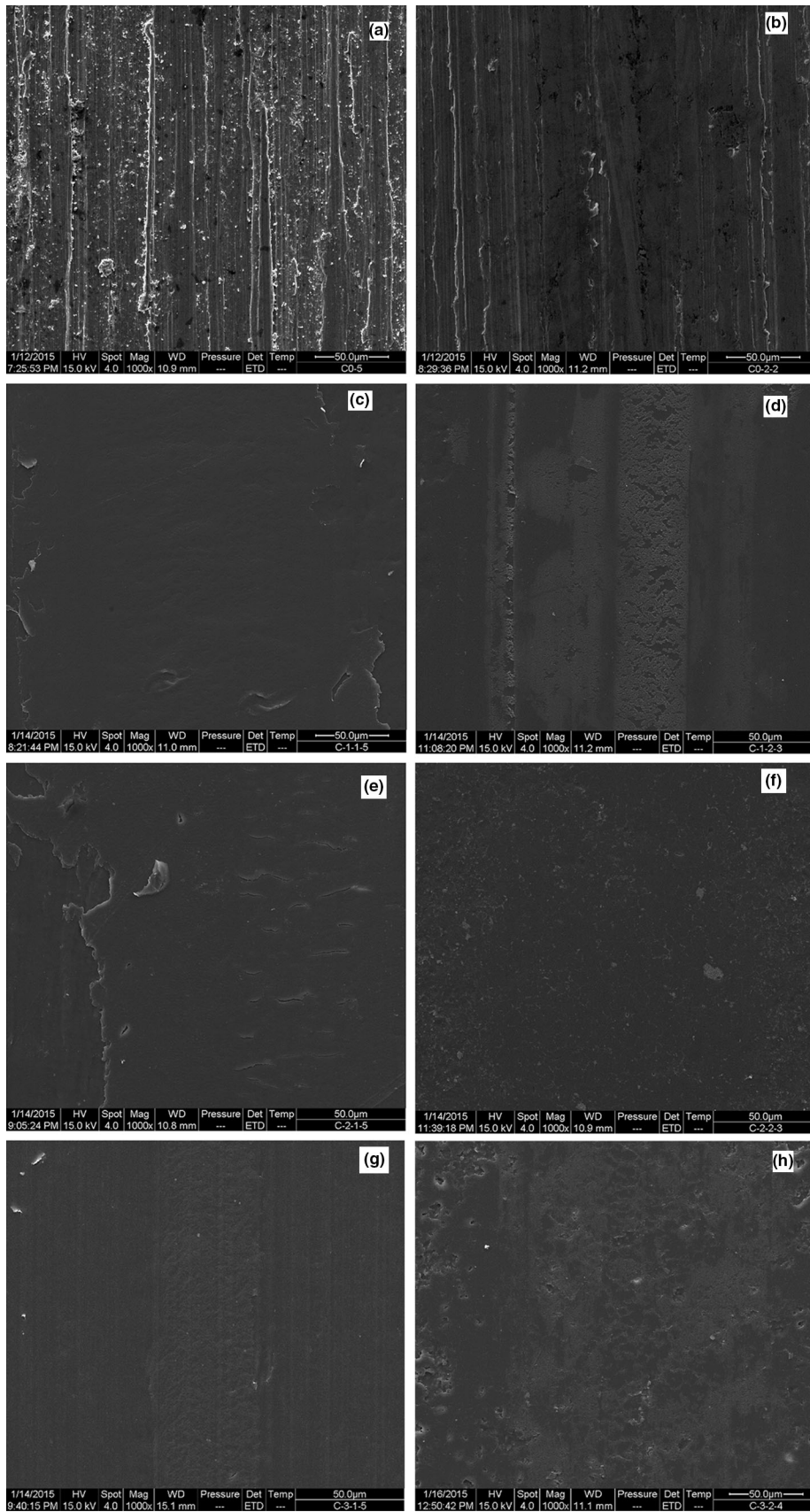


**Fig. 9** SEM micrographs of wear scar profiles for: (a) C0 in dry friction condition, (b) C0 in 25 wt.% NCS lubricated condition, (c) C1 in dry friction condition, (d) C0 in 25 wt.% NCS lubricated condition, (e) C2 in dry friction condition, (f) C0 in 25 wt.% NCS lubricated condition, (g) C3 in dry friction condition, and (h) C0 in 25 wt.% NCS lubricated condition



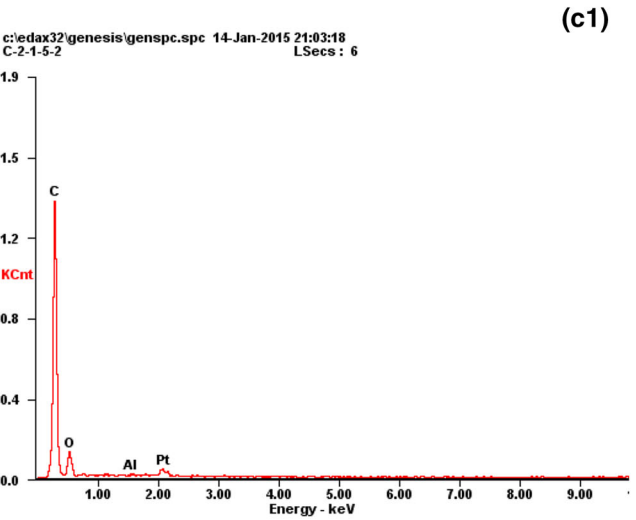
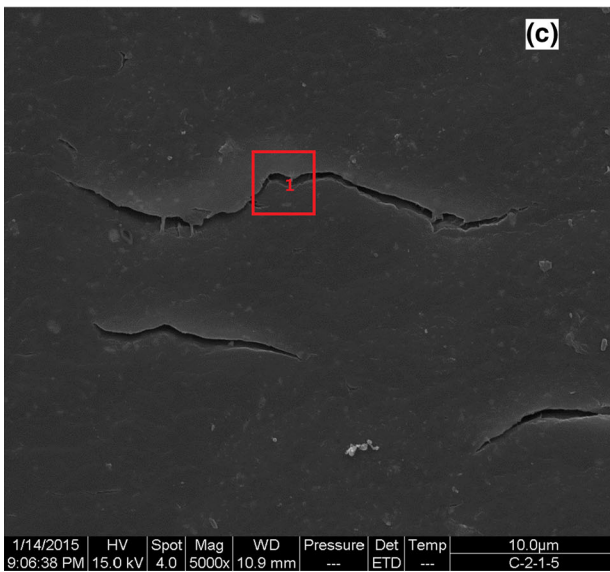
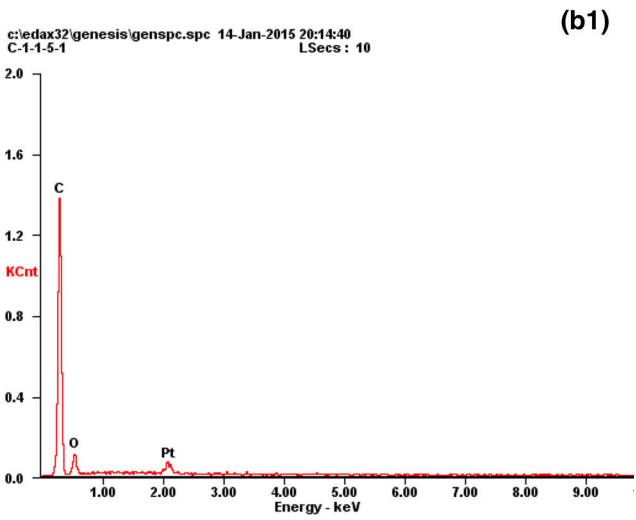
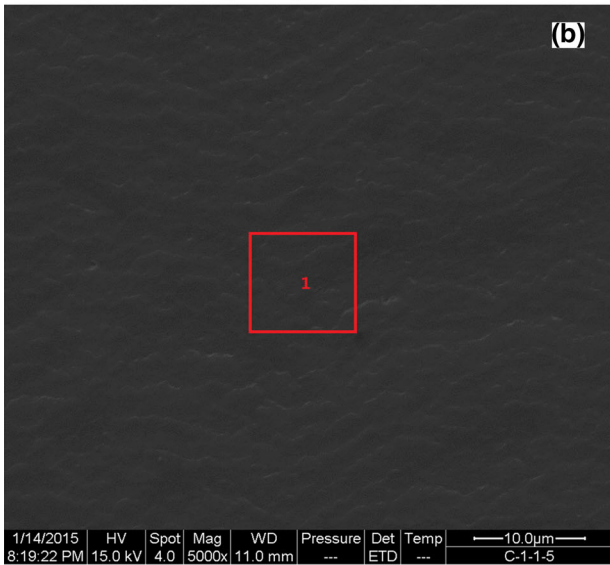
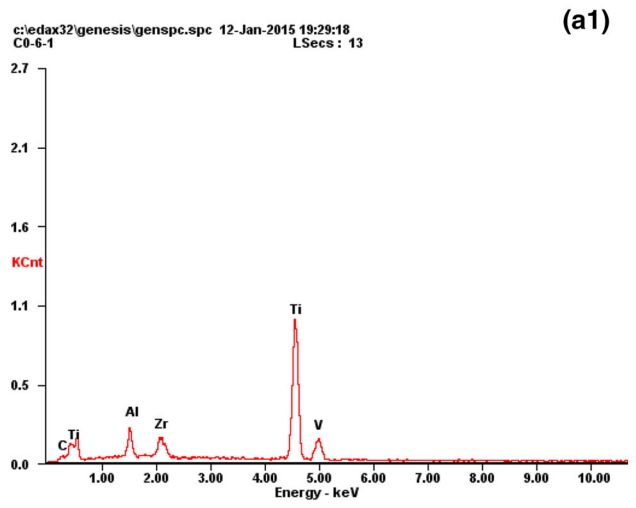
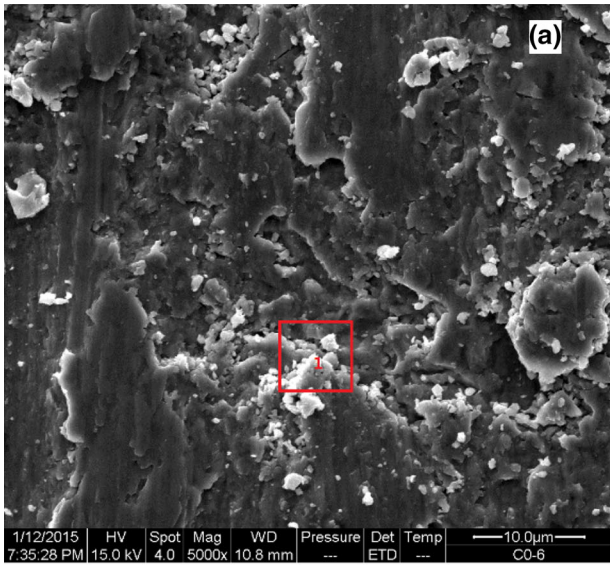


**Fig. 10** EDX analysis of wear scars for: (a) C0 in dry friction condition and (a1) relative EDX analysis, (b) C1 in dry friction condition and (b1) relative EDX analysis, (c) C2 in dry friction condition and (c1) relative EDX analysis, (d) C3 in dry friction condition and (d1) relative EDX analysis



(d1)

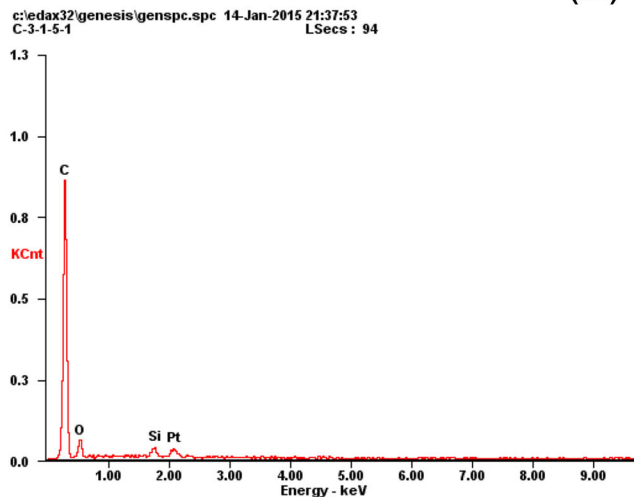


Fig. 10 continued

C2 and C3 are also composed of the coating materials mainly, without the elements of substrate as shown in Fig. 10(c1) and (d1) and 11(c1) and (d1). As for C2 sample, more fatigue cracks and adhesive area could be seen in Fig. 9(e) and 10(c). Therefore, it is suggested that fatigue wear and adhesive wear are the main wear mechanisms for C2 in dry friction condition. Moreover, it is noted that some adhesive wear debris are randomly scattered on the surface and no obvious wear scar could be found as shown in Fig. 9(f) and 11(c). The obtained results indicate that adhesive wear is the main wear mechanism for C2 in NCS lubricated condition. One can observe the presence of wear grooves and flake type wear debris on the worn surface of C3 shown in Fig. 9(g) and 10(d) but to a lesser degree, compared to C1 in the same condition. Yet, serious adhesive wear scar without distinct wear grooves are shown in Fig. 11(d). Hence, abrasive wear and adhesive wear are the main wear mechanisms for C3 in dry friction condition. While adhesive wear is the main wear mechanism for C3 in NCS lubricated condition.

### 3.4 Discussion

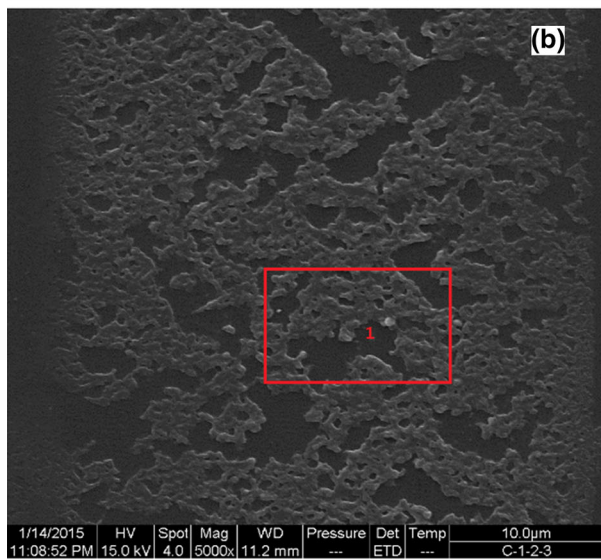
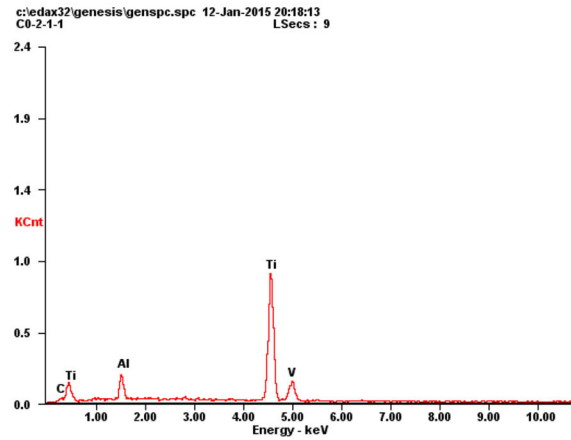
The tribological behaviors are some of the most important properties for titanium alloys in orthopedic applications. As mentioned above, owing to the better friction and wear resistances of PEEK and its composite materials (Ref 14), the tribological properties of Ti6Al4V alloy could be improved by PEEK and its composite coatings significantly. As a result, the friction coefficients, maximum wear width and maximum wear depth those coated Ti6Al4V alloy specimens decrease in comparison to bare Ti6Al4V samples both in dry friction and NCS lubricated conditions. Because of the low thermal conductivity of PEEK and its composite coatings (Ref 32), the friction-induced thermal effect in dry friction condition would lead to serious adhesion of wear debris. Consequently, there is a large amount of adhesive area and no obvious wear scars in the wear area of PEEK coatings shown in Fig. 9(c), (e), and (g). While in terms of bare Ti6Al4V alloy, owing to its excellent

thermal conductivity, the main wear mechanisms for bare Ti6Al4V alloy are the deformation under plowing force as well as abrasive wear and light adhesive wear in dry friction condition. Furthermore, the obtained results in the present study suggest that the tribological performances of PEEK composite coatings are better than that of pure PEEK coating. This may be attributed to the presence of Al<sub>2</sub>O<sub>3</sub>/SiO<sub>2</sub> nanoparticles, which are evenly distributed in PEEK coating. It is reported that a hard phase in the soft polymer matrix could decrease the coating deformation and true contact area with the counterbody under certain load (Ref 33). Therefore, these nanoparticles added into PEEK coatings could prevent the asperities of upper samples from penetrating the surfaces of PEEK, and relieve the deformation of the surfaces as well as the plowing effect. Also, due to the restriction of these nanoparticles, the macromolecule in the PEEK material could not prolapse easily. Furthermore, PEEK/Al<sub>2</sub>O<sub>3</sub> coating displays better tribological properties than PEEK/SiO<sub>2</sub> coating. The obtained results could be due to the different surface roughness values between the two sample surfaces. The surface of PEEK/Al<sub>2</sub>O<sub>3</sub> coating is smoother which could reduce the plowing effect under dry friction condition.

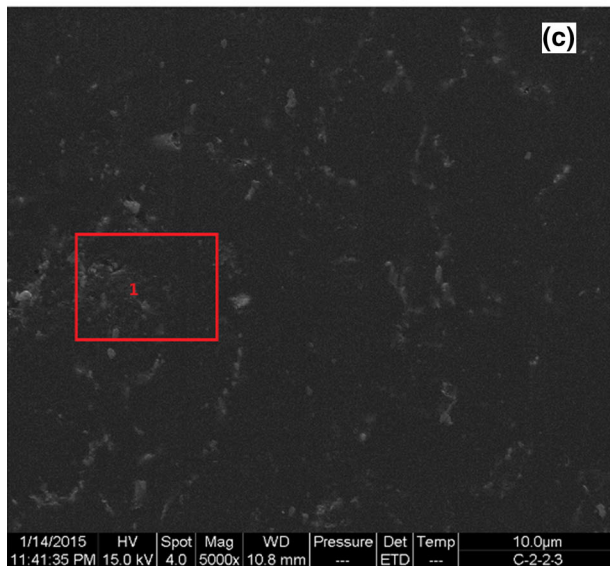
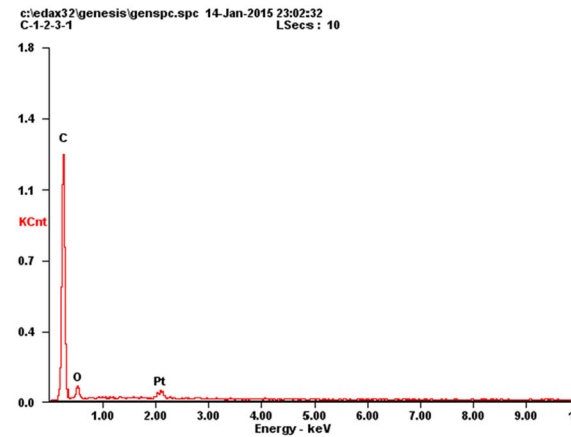
As far as NCS lubricated condition is concerned, a significant decrease in the friction coefficients and the maximum wear depth and width of PEEK and its composite coatings has been observed in the present study in comparison to dry sliding condition. It has been reported that there is a large amount of proteins in NCS (Ref 34), which could adsorb onto the surfaces of bare titanium alloy and PEEK coatings due to the excellent wettability. The adsorbed protein layer could reduce the direct contact between the ZrO<sub>2</sub> ball and the coatings and function as a semi-protective film (Ref 35). Therefore, the friction coefficients and wear rates are larger in dry friction condition than in NCS lubricated condition for both untreated and coated samples as shown in Fig. 6 and 7. According to literature (Ref 36), mixed lubrication and boundary lubrication may occur in simple daily activities for natural and artificial joints, because the film thickness can be very similar to the



(a1)



(b1)



(c1)

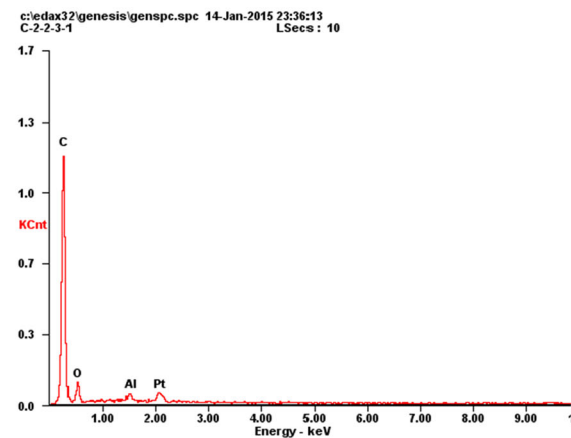


**Fig. 11** EDX analysis of wear scars for (a) C0 in 25 wt.% NCS lubricated condition and (a1) relative EDX analysis, (b) C1 in 25 wt.% NCS lubricated condition and (b1) relative EDX analysis, (c) C2 in 25 wt.% NCS lubricated condition and (c1) relative EDX analysis, (d) C3 in 25 wt.% NCS lubricated condition and (d1) relative EDX analysis



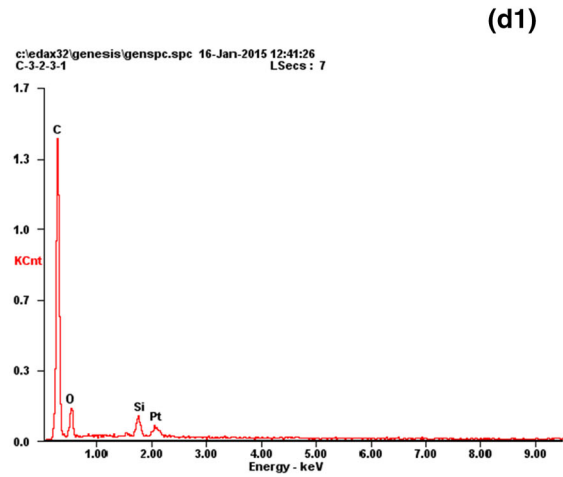
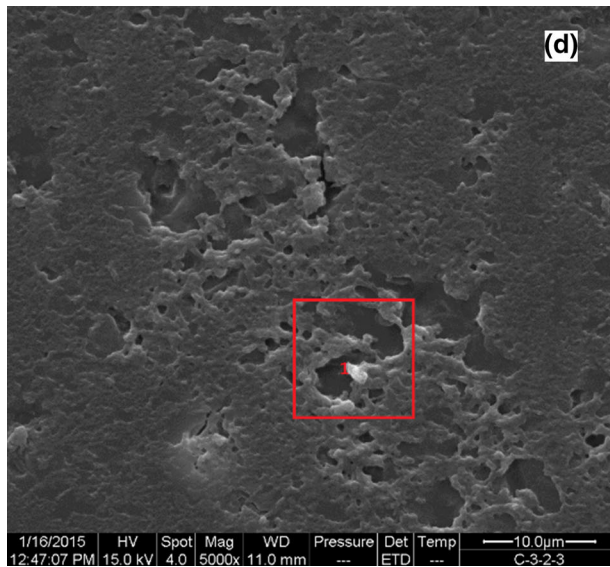


Fig. 11 continued

average roughness of the articulating surfaces. It is suggested that theoretical predictions of lubrication regimes are usually based on the  $\lambda$  ratio in Eq 1. The minimum film thickness  $h_{\min}$  could be evaluated by the well-known Hamrock-Dowson formula for isoviscous-elastic lubrication as shown in Eq 2.

$$\lambda = \frac{h_{\min}}{R'_q} \quad (\text{Eq 1})$$

$$\frac{h_{\min}}{R'_q} = 2.8 \left( \frac{\eta u_e}{E' R'} \right)^{0.65} \left( \frac{W_y}{E' R'^2} \right)^{-0.21} \quad (\text{Eq 2})$$

$$R' = \sqrt{R_{a1}^2 + R_{a2}^2} \quad (\text{Eq 3})$$

$$\frac{1}{R'} = \frac{1}{R_1} - \frac{1}{R_2} \quad (\text{Eq 4})$$

$$\frac{1}{E'} = \frac{1}{2} \left( \frac{1 - \nu_1^2}{E_1} + \frac{1 - \nu_2^2}{E_2} \right) \quad (\text{Eq 5})$$

In Eq 1 and 2,  $R'$ ,  $\eta$ ,  $u_e$ ,  $W_y$  and  $E'$  are the effective radius, the lubricant viscosity, the sliding velocity, the vertical load and the elastic modulus, respectively.  $R'_q$  in Eq 3 means the composite roughness. While in Eq 4 and 5,  $R_1$ ,  $E_1$ ,  $\nu_1$  and  $R_2$ ,  $E_2$ ,  $\nu_2$  are the radii, Young's modulus and Poisson ratio of the ball and the contacting material, respectively. According to the above equations,  $h_{\min}$  is about 573 nm in this study. Therefore, under NCS lubricated condition, the  $\lambda$  ratio for PEEK/ $\text{Al}_2\text{O}_3$  coating is about 1.045 and that for PEEK/ $\text{SiO}_2$  coating is 0.679. Once the  $\lambda$  ratio is evaluated, lubrication regime could be conventionally identified by the following ranges: (a)  $0.1 < \lambda < 1$ : boundary lubrication, (b)  $1 \leq \lambda < 3$ : mixed lubrication, and (c)  $\lambda \geq 3$ : full film lubrication. Thus,

under NCS lubricated condition, PEEK/ $\text{Al}_2\text{O}_3$  coating is mixed lubrication, while PEEK/ $\text{SiO}_2$  coating is boundary lubrication. It is suggested that the mixed or boundary lubrication film has formed with the improvement of wettability, which will influence the friction and wear under lubrication (Ref 37). It is reported that the protein adsorption displays a strong friction under mixed lubrication while a low friction under boundary lubrication (Ref 37, 38). These are inconsistent with results shown in Fig. 3 and 6(b). Hence, the friction coefficient of C3 is the lowest. Besides, the presence of hydroxyl groups found in the introduced  $\text{Al}_2\text{O}_3/\text{SiO}_2$  nanoparticles (Ref 39), also helps in reducing the adhesion between the sliding materials. The previous results have indicated that these hydroxyl groups tend to reduce the direct contact between bearing materials under NCS lubricated conditions (Ref 40). Hence, compared with those of pure PEEK coating, the wear volumes are reduced, which is similar to the conclusion of Kuo et al. (Ref 41). Because of the adsorbed proteins, the wear debris is able to get adhered on the surface easily. Thus, adhesive wear is one of the operative wear mechanisms for these samples in NCS lubricated condition. Therefore, better lubricated condition of PEEK/ $\text{Al}_2\text{O}_3$  coating leads to the optimum wear behavior under NCS lubricated condition.

## 4. Conclusions

Different PEEK composite coatings were studied under unlubricated and 25 wt.% NCS lubricated conditions. Based on their surface layer characterization and tribological characteristics, the following major conclusions could be obtained.

1. The contact angle values of PEEK composite materials coated Ti6Al4V alloys were all higher than those of the bare sample. Meanwhile, the static contact angle values with distilled water were larger than those with 25 wt.% NCS because of the adsorption of proteins.
2. Micro-hardness values of PEEK composite coatings decreased significantly, compared with that of bare Ti6Al4V

alloy. The high hardness of SiO<sub>2</sub> resulted in the highest micro-hardness of PEEK/SiO<sub>2</sub> coating ( $27.7 \pm 3.1$  HV) among the three coatings.

3. The tribological performances of PEEK composite coatings were better than that of pure PEEK coating. This has been attributed presence of Alumina and Silica nanoparticles, which were evenly distributed in PEEK coating. These nanoparticles prevented the asperities of upper samples from penetrating the surfaces of PEEK, and relieved the deformation of the surfaces as well as the plowing effect.
4. Under the conditions used in the present study, PEEK/Al<sub>2</sub>O<sub>3</sub> composite coating demonstrated optimum tribological properties and hence, could be taken as a potential candidate to be applied as bearing material for artificial cervical disk.

## Acknowledgment

This project was supported by the China Postdoctoral Science Foundation (Grant No. 2015M580735) and the Economy, Trade and Information Commission of Shenzhen Municipality (Grant No. SMJKPT20140417010001). The work is also financially supported by the National Natural Science Foundation of China (Grant No. 51522504). We are grateful to Chun ZHAO, president of Beijing Sino-Rich Material Technology Co., Ltd, for his kindly help of the PEEK composite coatings preparation for us.

## Conflict of Interest

We declare that we have no conflict of interest.

## References

1. M. Niinomi, M. Nakai, and J. Hieda, Development of New Metallic Alloys for Biomedical Applications, *Acta Biomater.*, 2012, **8**, p 3888–3903
2. T.M. Grupp, H. Meisel, J.A. Cotton, J. Schwiesau et al., Alternative Bearing Materials for Intervertebral Disc Arthroplasty, *Biomaterials*, 2010, **31**, p 523–531
3. C. Zhang, Y. Liu, S. Wen, and S. Wang, Poly(vinylphosphonic acid) (PVPA) on Titanium Alloy Acting as Effective Cartilage-Like Superlubricity Coatings, *Acs Appl. Mater. Inter.*, 2014, **6**(20), p 17571–17578
4. S. Wang, Z. Liao, Y. Liu, and W. Liu, Different Tribological Behaviors of Titanium Alloys Modified by Thermal Oxidation and Spraying Diamond Like Carbon, *Surf. Coat. Technol.*, 2014, **252**, p 64–73
5. M.P. Ananth and R. Ramesh, Reciprocating Sliding Wear Performance of Hard Coating on Modified Titanium Alloy Surfaces, *Tribol. Trans.*, 2015, **58**, p 169–176
6. M.P. Ananth and R. Ramesh, Tribological Improvement of Titanium Alloy Surfaces Through Texturing and TiAlN Coating, *Surf. Eng.*, 2014, **30**, p 758–762
7. X. Guan, Z. Lu, and L. Wang, Achieving High Tribological Performance of Graphite-Like Carbon Coatings on Ti6Al4V in Aqueous Environments by Gradient Interface Design, *Tribol. Lett.*, 2011, **44**, p 315–325
8. Q. Wang, F. Zhou, Z. Zhou, Y. Yang et al., Influence of Ti Content on the Structure and Tribological Properties of Ti-DLC Coatings in Water Lubrication, *Diam. Relat. Mater.*, 2012, **25**, p 163–175
9. X. Feng and Y. Xia, Tribological Properties of Ti-Doped DLC Coatings Under Ionic Liquids Lubricated Conditions, *Appl. Surf. Sci.*, 2012, **258**, p 2433–2438
10. Z. Yang, D. Wu, and M. Liu, Electroless Ni-P-PTFE Composite Coatings on Titanium Alloy and Their Tribological Properties, *Adv. Mater. Res.*, 2011, **291–294**, p 12–17
11. B. Panjwani, N. Satyanarayana, and S.K. Sinha, Tribological Characterization of a Biocompatible Thin Film of UHMWPE on Ti6Al4V and the Effects of PFPE as Top Lubricating Layer, *J. Mech. Behav. Biomed.*, 2011, **4**, p 953–960
12. Y. Luo, S. Ge, Z. Jin, and J. Fisher, Effect of Surface Modification on Surface Properties and Tribological Behaviours of Titanium Alloys, *Proc. Inst. Mech. Eng. Part J*, 2009, **223**, p 311–316
13. S.H. Modi, K.B. Dikovics, H. Gevgilili, G. Mago et al., Nanocomposites of Poly(ether ether ketone) with Carbon Nanofibers: Effects of Dispersion and Thermo-oxidative Degradation on Development of Linear Viscoelasticity and Crystallinity, *Polymer*, 2010, **51**, p 5236–5244
14. F. Rose and R. Oreffo, Bone Tissue Engineering: Hope vs Hype, *Biochem. Biophys. Res. Commun.*, 2002, **292**, p 1–7
15. H. Zhou, V.K. Goel, and S.B. Bhaduri, A Fast Route to Modify Biopolymer Surface: A Study on Polyetheretherketone (PEEK), *Mater. Lett.*, 2014, **125**, p 96–98
16. O.E. Pohler, Unalloyed Titanium for Implants in Bone Surgery, *Injury*, 2000, **31**, p D7–D13
17. E.E. Nunez, S.M. Yeo, K. Polychronopoulou, and A.A. Polycarpou, Tribological Study of High Bearing Blended Polymer-Based Coatings for Air-Conditioning and Refrigeration Compressors, *Surf. Coat. Technol.*, 2011, **205**, p 2994–3005
18. S. Wang, Z. Liao, Y. Liu, and W. Liu, Influence of Thermal Oxidation Temperature on the Microstructural and Tribological Behavior of Ti6Al4V Alloy, *Surf. Coat. Technol.*, 2014, **240**, p 470–477
19. X. Hou, C.X. Shan, and K. Choy, Microstructures and Tribological Properties of PEEK-Based Nanocomposite Coatings Incorporating Inorganic Fullerene-Like Nanoparticles, *Surf. Coat. Technol.*, 2008, **202**, p 2287–2291
20. L. Yan, J. Wang, X. Han, Y. Ren et al., Enhanced Microwave Absorption of Fe Nanoflakes After Coating with SiO<sub>2</sub> Nanoshell, *Nanotechnology*, 2010, **21**, p 95708
21. C.K. Akkan, M.E. Hammadeh, A. May, H. Park et al., Surface Topography and Wetting Modifications of PEEK for Implant Applications, *Laser Med. Sci.*, 2014, **29**, p 1633–1639
22. C. Matschegewski, S. Staehlke, R. Loeffler, R. Lange et al., Cell Architecture–Cell Function Dependencies on Titanium Arrays with Regular Geometry, *Biomaterials*, 2010, **31**, p 5729–5740
23. P.R. Pandey and S. Roy, Is it Possible to Change Wettability of Hydrophilic Surface by Changing Its Roughness, *J. Phys. Chem. Lett.*, 2013, **4**, p 3692–3697
24. C.N. Elias, Y. Oshida, J.H.C. Lima, and C.A. Muller, Relationship between Surface Properties (Roughness, Wettability and Morphology) of Titanium and Dental Implant Removal Torque, *J. Mech. Behav. Biomed.*, 2008, **1**, p 234–242
25. G. Zhang, H. Liao, H. Yu, V. Ji et al., Correlation of Crystallization Behavior and Mechanical Properties of Thermal Sprayed PEEK Coating, *Surf. Coat. Technol.*, 2006, **200**, p 6690–6695
26. R. Xu, J. Wang, L. He, and Z. Guo, Study on the Characteristics of Ni–W–P Composite Coatings Containing Nano-SiO<sub>2</sub> and Nano-CeO<sub>2</sub> Particles, *Surf. Coat. Technol.*, 2008, **202**, p 1574–1579
27. T. Palathai, J. Tharajak, and N. Sombatsompop, Hardness, Adhesion Index and Microstructure of PEEK Coating on Al or Fe Substrate by LVOF Flame Spray, *Mater. Sci. Eng. A*, 2008, **485**, p 66–73
28. G. Zhang, H. Yu, C. Zhang, H. Liao, and C. Coddet, Temperature Dependence of the Tribological Mechanisms of Amorphous PEEK (Polyetheretherketone) Under Dry Sliding Conditions, *Acta Mater.*, 2008, **56**, p 2182–2190
29. S.R. Ge, Q.L. Wang, D.K. Zhang, H. Zhu et al., Friction and Wear Behavior of Nitrogen Ion Implanted UHMWPE Against ZrO<sub>2</sub> Ceramic, *Wear*, 2003, **255**, p 1069–1075
30. C.L. Brackett, G. John, S. Williams, Z. Jin et al., Wear of Ceramic-on-Carbon Fiber-Reinforced Poly-ether Ether Ketone Hip Replacements, *J. Biomed. Mater. Res. B*, 2012, **100B**, p 1459–1465
31. S.C. Scholes and A. Unsworth, Pitch-Based Carbon-Fibre-Reinforced Poly(ether-ether-ketone) OPTIMA (R) Assessed as a Bearing Material in a Mobile Bearing Unicondylar Knee Joint, *Proc. Inst. Mech. Eng. Part H*, 2009, **223**, p 13–25
32. X. Huang, P. Jiang, and T. Tanaka, A Review of Dielectric Polymer Composites with High Thermal Conductivity, *IEEE Ind. Electron. Mag.*, 2011, **27**, p 8–16
33. G. Zhang, H. Liao, H. Li, C. Mateus et al., On Dry Sliding Friction and Wear Behaviour of PEEK and PEEK/SiC-Composite Coatings, *Wear*, 2006, **260**, p 594–600

34. M. De Buck, M. Gouwy, P. Proost, S. Struyf, and J. Van Damme, Identification and Characterization of MIP-1 $\alpha$ /CCL3 Isoform 2 from Bovine Serum as a Potent Monocyte/Dendritic Cell Chemoattractant, *Biochem. Pharmacol.*, 2013, **85**, p 789–797
35. J. Huang, L. Wang, B. Liu, S. Wan, and Q. Xue, In Vitro Evaluation of Tribological Response of Mo Doped GLC Film in Different Biological Mediums, *Acs Appl. Mater. Inter.*, 2015, **7**(4), p 2772–2783
36. L. Mattei, F. Di Puccio, B. Piccigallo, and E. Ciulli, Lubrication and Wear Modelling of Artificial Hip Joints: A Review, *Tribol. Int.*, 2011, **44**, p 532–549
37. S. Wang, Y. Liu, C. Zhang, Z. Liao, and W. Liu, The Improvement of Wettability, Biotribological Behavior and Corrosion Resistance of Titanium Alloy Pretreated by Thermal Oxidation, *Tribol. Int.*, 2014, **79**, p 174–182
38. R.M. Hall and A. Unsworth, Friction in Hip Prostheses, *Biomaterials*, 1997, **18**, p 1017–1026
39. P. Thissen, T. Peixoto, R.C. Longo, W. Peng et al., Activation of Surface Hydroxyl Groups by Modification of H-Terminated Si (111) Surfaces, *J. Am. Chem. Soc.*, 2012, **134**, p 8869–8874
40. M. Palacio and B. Bhushan, A Review of Ionic Liquids for Green Molecular Lubrication in Nanotechnology, *Tribol. Lett.*, 2010, **40**, p 247–268
41. M.C. Kuo, C.M. Tsai, J.C. Huang, and M. Chen, PEEK Composites Reinforced by Nano-sized SiO<sub>2</sub> and Al<sub>2</sub>O<sub>3</sub> Particulates, *Mater. Chem. Phys.*, 2005, **90**, p 185–195